Japan Geoscience Union Meeting 2013
(May 19-24 2013 at Makuhari, Chiba, Japan)

SSS28-01 Room:303 Time:May 22 16:15-16:30

An arithmetic geometrical approach for modeling of seismic activity

Hiroyuki Fujiwara[1*]

[1]NIED

Earthquake occurs in a discrete manner in time and space. Except for the main shock-aftershock sequences, earthquakes that seem to be individually independent. However, when viewed as a whole, we find that there are laws, for example, G-R law, that govern the entire earthquakes that seem to be individually independent.

A similar phenomenon can be observed also in the world of ”number”. The most basic example is the distribution of the prime numbers in integers. The presence of interesting relationships, for example, the reciprocity law of quadratic residue, has been found in prime numbers that seem to be individually independent. Class field theory as a theoretical system relates to the structure of the number has been established. In addition, a lot of knowledge is going to be achieved in recent years by the development of arithmetic geometry that regards ”number” as geometric objects. Arithmetic geometry was developed by applying the theory of scheme to ”number”, which was developed in algebraic geometry aimed to study algebraic varieties consisting of zeros of polynomials. Arithmetic geometry have revealed interesting laws that govern the world of the ”number”.

We consider the correspondence as follows to the world of ”number” and ”earthquake” that seem to be completely independent. Let p_i be the i-th prime and take appearance interval of prime, p_i-p_{i-1}, as index of i-th prime. Let e_i be the i-th earthquake, T(e_i) be occurrence time of the i-th earthquake, and M_o(e_i) be moment of the i-th earthquake. We assume that the following equations hold.

T(e_i)=p_i,

log(M_o(e_i))=p_i-p_{i-1}

By performing numerical experiments, we have found that the characteristics of this correspondence are similar to the G-R law. We call the model obtained by this correspondence as ”arithmetical seismic activity model”.

Based on these considerations, we can regard the ”arithmetical seismic activity model” as an object of the scheme theory. By using knowledge from the arithmetic geometry, it is expected to obtain knowledge about laws that control seismic activity. We have an image of earthquakes that fracture starts from a point in space that does not have infinite special boundary conditions and expand gradually to the destruction of the entire area. Although it is believed that the boundary conditions more realistic for the physical model, we expect to be able to handle them by considering to limit or to extend the ”number” and those are objects of the scheme theory. By using the ”arithmetical seismic activity model”, the unresolved issue on the math as ”the twin primes exist infinitely” is replaced by the problem of the nature of the seismic activity, such that the smallest earthquakes occur infinitely.

Keywords: prime, arithmetic geometry, Gutenberg-Richter relation, earthquake

Japan Geoscience Union Meeting 2013
(May 19-24 2013 at Makuhari, Chiba, Japan)

SSS28-02 Room:303 Time:May 22 16:30-16:45

Development of an epicenter estimation method using 3D polarity and its application to dynamic triggering events

Takahiko Uchide[1*]

[1]Disaster Prevention Research Institute, Kyoto University

Recently based on the development of seismic observations and computational resources, many methods to locate earthquakes with unclear P and S onset, such as low-frequency earthquakes and dynamic triggering earthquakes, have been proposed [e.g., Obara, 2002; Kao et al., 2005; Shelly et al., 2007].

Here I show a new method to estimate epicenters using the polarities of seismograms. The basic idea is as follows: First, we detect rectilinear signal from seismograms; then assuming such rectilinear waveforms are P waves and the polarization direction is same as the back azimuth, we estimate epicenters directed by multiple stations. This kind of strategy is often used to confirm hypocenter determinations with few stations. This study carries out this procedure automatically. The test field of this study is Hida region, Central Japan. The goal of this paper is so far to detect more events dynamically triggered by the 2011 Tohoku earthquake than those detected by manual process [Miyazawa, 2011].

I apply a polarization analysis method using analytic signal (its real and imaginary parts are an original signal and its Hilbert transform, respectively) of both horizontal and vertical components [Vidale, 1986]. We construct a variance-covariance matrix $\boldsymbol{C}(t)$ of the analytic signal at each time. Its eigenvector corresponding to the largest eigenvalue represents the polarization direction. The use of the moving average of data will stabilize the analysis. The strength of the polarization is represented by $P_s = 1 - (a_2 + a_3)/a_1$, where $a_1 > a_2 > a_3$ are the eigenvalues of $\boldsymbol{C}(t)$. If the polarization direct is downward, we change it to an upward one by changing the sign of dip angle and taking 180 degrees opposite of the azimuth.

In a realistic case, the polarization direction and back azimuth are not exactly same, because (1) the horizontal heterogeneity of seismic velocity structure and (2) the misorientation of seismometers. Those directions also differs, when (3) other phases such as S waves are analyzed. In case of (3), it is less probable that multiple stations indicate the same point. To check the effect of (1) and (2) quantitatively, I calculate the differences between the back azimuth and the polarization direction of seismograms for 0.5 s from P arrivals, from the phase information in the JMA unified earthquake catalog, from earthquakes in Hida region. At most of stations, the average and the standard deviation of them are within 5 degrees and 5 to 10 degrees, respectively, though at some stations the average is much larger, probably due to the misorientation of seismometers.

Based on the time history of the polarities, epicenters are searched by a grid-search manner, taking account of (a) travel time of P waves from a grid to stations, (b) difference between the polarization direction and azimuths from stations to a grid, and (c) the strength of the polarity P_s. I construct an evaluation function to search for an epicenter location and origin time.

This method is applied to single M2-class earthquakes in the Hida region using velocity seismograms from Hi-net and DPRI seismic network. The data is high-pass filtered at 4 Hz. The epicenters determined by my method are close to those of JMA unified catalog. When I analyze an earthquake outside of the network, ghost errors are seen.

Finally I apply this method to seismic data in the Hida region during seismic waves from the 2011 Tohoku earthquake are passing. The velocity seismograms are high-pass filtered at 4 Hz. Many events are detected. Some of them correspond to events detected by Miyazawa [2011], but some of them are not in his catalog.

This study will improve the catalog of dynamic triggering earthquakes and promotes the dynamic triggering studies. Moreover this method will contribute to other type of seismological studies, such as automatic data processing and structure studies.

Keywords: Epicenter determination method, 3D polarity of motion, Hida, Dynamic triggering of earthquakes, the 2011 Tohoku earthquake

Japan Geoscience Union Meeting 2013
(May 19-24 2013 at Makuhari, Chiba, Japan)

SSS28-03 Room:303 Time:May 22 16:45-17:00

Theoretical background of back-projection imaging and its relation to time-reversal and inverse solutions

Yukitoshi Fukahata[1*], Yuji Yagi[2], RIVERA, Luis[3]

[1]DPRI, Kyoto University, [2]Life and Environ. Sci., Univ. Tsukuba, [3]EOST, University of Strasbourg

The back-projection (BP) method has become a popular tool to image the rupture process of large earthquakes since the success of Ishii et al. (2005), while it has not been clear what the BP image represents physically. We clarified the theoretical background of the back-projection (BP) imaging and related it to classical inverse solutions via the hybrid back-projection (HBP) imaging (Yagi et al., 2012). In the HBP method, which is mathematically almost equivalent to the time-reversal imaging, cross correlations of observed waveforms with the corresponding Green's functions are calculated. The key condition for BP to work well is that the Green's function is sufficiently closer to the delta function after stacking. Then, we found that the BP image represents the slip motion on the fault, and approximately equals to the least squares solution. In HBP, instead of the Green's function in BP, the stacked auto-correlation function of the Green's function must be close to the delta function to obtain a fine image. Because the auto-correlation function is usually closer to the delta function than the original function, we can expect that HBP works better than BP, if we can reasonably estimate the Green's function. With another condition that the stacked cross-correlation function of the Green's functions for different source locations is small enough, the HBP image is approximately equal to the least squares solution. If these assumption are not satisfied, however, the HBP image corresponds to a damped least squares solution with an extremely large damping parameter, which is clearly inferior to usual inverse solutions. We show some simple examples of numerical computation to check the validity of the above mentioned conditions implicitly assumed in the BP and HBP methods.

Keywords: Back projection, Time reversal, Inversion, least squares solution

Japan Geoscience Union Meeting 2013
(May 19-24 2013 at Makuhari, Chiba, Japan)

SSS28-04 Room:303 Time:May 22 17:00-17:15

Nondimensional Controlling Parameter about Inelastic Porosity Evolution Law and its Effect on Dynamic Earthquake Slip

Takehito Suzuki[1*], Teruo Yamashita[2]

[1]EPS, Univ. Tokyo, [2]ERI, Univ. Tokyo

In a series of our studies, we have studied effects of the interaction among effects of shear heating, fluid pressure and inelastic pore creation on dynamic fault slip and found two nondimensional controlling parameters Su and Su' about the interaction for one-dimensional (1-D) fault model. The parameter Su represents the relative dominance of the effect of inelastic pore creation on the fluid pressure change over that of shear heating, while Su' is associated with the dominance of fluid flow effect over the effect of shear heating. We have succeeded in explaining many aspects of dynamic earthquake slip behavior in a unified way on the basis of the parameters: for example, ordinary earthquakes and slow earthquakes are understood in terms of those parameters.

However, there is a problem in our modeling that we have assumed too simple form of inelastic porosity evolution; inelastic porosity change rate was assumed to be proportional to slip velocity. Porosity in natural faults is suggested to have an upper limit, phi_{inf}, by observational and experimental studies. The framework the authors have employed assumes that porosity change, phi, is negligibly smaller than the upper limit.

We introduce the third nondimensional parameter, Su^{ul}, to describe the effect of the upper limit of inelastic porosity. We neglect here fluid flow; that is, Su'=0. If we assume Su>1, fluid pressure decrease due to inelastic pore creation at an initial stage of slip reduces slip velocity. After the initial stage, two qualitatively different behaviors of slip appear. For some parameter ranges of Su and Su^{ul}, slip accelerates and the slip velocity approaches to a positive constant value. This behavior occurs because phi approximately approaches to phi_{inf} and effect reducing the fluid pressure (and the slip velocity) due to pore creation vanishes. In this case, shear stress acting on a fault plane is completely released at the final stage due to thermal pressurization. On the other hand, for the other ranges, slip velocity approximately approaches to zero and the slip ceases spontaneously because phi is so small that the effect of phi_{inf} does not appear. Both high speed slip and spontaneous slip cessation can be understood in a single framework in the present model.

We also found that two important governing porosities, phi_1* and phi_2*, exist in the present model and succeeded in obtaining their analytical forms in terms of Su and Su^{ul}. The value phi_f*, defined as the value of normalized inelastic porosity phi$*$ after an infinitely long time, cannot take values between phi_1* and unity at the stable state (situation where phi$*$ is unity represents phi equals to the upper limit) because if phi$*$ approaches to phi_1*, the slip accelerates and phi_f* takes a value unity. The porosity phi_1* can be regarded as the critical value distinguishing the system behavior, slip acceleration and spontaneous slip cessation. In addition, the value of phi_f* cannot take values smaller than phi_2*, which is related to thermal energy generation. Observed porosity can be an indicator of thermal energy.

Keywords: heat, fluid pressure, inelastic porosity, high speed slip, spontaneous slip cessation

Japan Geoscience Union Meeting 2013
(May 19-24 2013 at Makuhari, Chiba, Japan)

SSS28-05 Room:303 Time:May 22 17:15-17:30

Development of extended BIEM and its application to earthquake dynamic rupture analysis in inhomogeneous media

Tetsuya Kusakabe[1*], Nobuki Kame[1]

[1]Earthquake Res. Inst., Univ. of Tokyo

The boundary integral equation method (BIEM) has been applied to the analysis of rupture propagation of non-planar faults in an unbounded homogeneous elastic medium. We have proposed an extended BIEM (XBIEM) that is applicable in an inhomogeneous bounded medium consisting of homogeneous sub-regions (Kame and Kusakabe, 2012). We have developed a preliminary code for mode III dynamic rupture propagation interacting with medium interfaces. The validation tests have been carried out by comparing the XBIEM results with the BIEM solution for simple problems of the wave propagation and the dynamic rupture in a homogeneous full-space with a planar interface. It was found out that the discretized interfaces worked well for both problems.

In the present paper, we additionally validated our numerical code for two specific cases: 1) wave propagation in a homogeneous media with a non-planar interface and 2) wave propagation in a bimaterial with a planar interface. For the first case, it was found out that non-planar interface worked quite well. For the second case, our numerical result showed a good agreement with Hirano's analytic solution (Hirano, private communication). In both cases, our numerical code worked well enough and we proceed to apply our code to a new type of problem: dynamic rupture propagation interacting with a medium interface.

Here we considered dynamic rupture propagation on a planar fault embedded normal to the planar interface of a bimaterial. Spontaneous rupture is allowed not only on the planar main fault but also on the interfacial fault and it is controlled by slip-weakening laws on them: their peak strength are separately chosen and its ratio zeta=tauˆpeak_main/tauˆpeak_interface is chosen as one of controlling parameters. Another parameter is eta chosen as a ratio of the shear wave velocities, eta=beta_+/beta_-. Simulations were conducted for hundreds of parameter sets of (eta, zeta). Our results showed two distinct rupture processes: a) one is to propagate rupture just on the prescribed fault, and b) another is to activate the subsidiary interfacial rupture, which finally results in arresting rupture on the main planar fault.

Two processes were found to be clearly divided by a line in the parameter plane (eta, zeta). With increasing zeta, rupture tends to stay on the main fault with less significant activation of subsidiary interfacial rupture and it agrees with our physical anticipation. With increasing eta from 0.7 to 1.3 (one means homogeneous), rupture process shifts from (a) to (b). This eta dependency is not easily understandable at this moment but it clearly showed a significant effect of inhomogeneous medium on arresting dynamic rupture.

Keywords: dynamic rupture, BIEM, bimaterial interface, simulation

Japan Geoscience Union Meeting 2013
(May 19-24 2013 at Makuhari, Chiba, Japan)

SSS28-06 Room:303 Time:May 22 17:30-17:45

3D dynamic rupture simulation of a subducting reverse fault and its branch fault

Shintaro Tamura[1*], Satoshi Ide[1]

[1]Univ. of Tokyo, EPS

The Mw 9.0 Tohoku-Oki earthquake hit the northeast Japan on March 11, 2011 generating huge strong motion and tsunami and the area with the largest slip amount was located near the Japan Trench. Exploring the dynamics of the Tohoku-Oki earthquake is important for understanding physics of mega-thrust earthquakes and estimating the probability of rupture extensions or tsunami geneses to prevent future disasters. We model a shallow dipping mega-thrust earthquake on a bi-material interface with a free surface by using a 3D finite element method to solve elastodynamic equations and a slip-weakening friction law on the fault plane. As a preliminary study, we simulate in the relatively simple situations with a planar fault and a homogeneous prestress. Reflected body waves from the free surface strongly affect the normal and shear stress on the fault, and both the normal and the shear stress decrease just after the rupture reaches the trench. The slip on the fault reflects at the trench and rapidly propagates downward at the P-wave velocity. This downward reflected slip is consistent with the west-northwest directivity of the Tohoku-Oki earthquake. Final slip distribution with largest slip at the trench is also consistent with some kinematic slip models. Deformation style of the free surface changes depending on the dip angle and material contrast. The amount of vertical motion of the hanging wall is larger for the case of more compliant hanging wall and much larger than that of the footwall. Our simulations suggest that the huge tsunami is generated due to large amount of the surface deformation which is enhanced in the wedge part of the compliant hanging wall.

Keywords: dynamic rupture modeling in a subduction zone, branch fault, plastic yielding, FEM

Japan Geoscience Union Meeting 2013
(May 19-24 2013 at Makuhari, Chiba, Japan)

SSS28-07 Room:303 Time:May 22 17:45-18:00

Difference in the seismic rupture process between slow tsunami and megathrust earthquakes

Yuji Yagi[1*], Yuta Mitsui[2], Hayaki Ezaki[1]

[1]Life and Env. Sci., Univ. of Tsukuba, [2]Sci., Hokkaido Univ.

After the 2011 Tohoku earthquake, we know that huge co-seismic slip can occur at shallow part of subduction zone where slow tsunami earthquakes have been detected (e.g. the 1986 Meiji-Sanriku earthquake). To understand the nature of megahrust earthquakes as well as slow tsunami earthquakes, it is important to investigate the slip behavior in the area. We estimated the spatio-temporal slip-rate distribution of megathrust and slow tsunami earthquakes using a novel seismic source inversion method (Yagi and Fukahata, 2011, GJI) and a Hybrid Back-projection method (Yagi et al., 2012, EPSL), and then compared the observation results to simulation results. We inverted and projected the slip-rate function on fault for the 1992 Nicaragua slow tsunami earthquake, the 2006 Java slow tsunami earthquake, the 2010 Mentawai slow tsunami earthquake, and the 2011 Tohoku megathrust earthquake. In the case of slow tsunami earthquakes, we found a smooth and slow slip (~0.1m/s) that continued over 50 s near the trench, while pulse-like slip was detected in and around the main-shock hypocenter. In the case of the 2011 Tohoku megathrust earthquake, we also found a smooth and fast slip (~1.0 m/s) that continued over 80 s near the trench. The slow tsunami and megathrut earthquakes have a release of seismic energy in the downdip area that triggered smooth slip in the updip area. The difference of slip-rate between the analyzed slow tsunami earthquakes and Tohoku megathrust earthquake may suggest the existence of a non-linear rupture characteristic in the shallowest megathrust faults. Next, we performed dynamic rupture simulations using simplified fault models and the mechanism of thermal fluid pressurization. We found that small fluctuations of initial shear stress near the trench, within 1 MPa, lead to differences in seismic moment release greater than two orders of magnitude. Moderate slip events with trapezoidal source time functions appear to occupy a transition position, between shallow megathrust earthquakes, with surface rupture, and smaller ordinary earthquakes, without surface rupture. We interpret this result as representing the differences in interplate slip between shallow megathrust earthquakes, tsunami earthquakes, and ordinary earthquakes in the same region. The observation and numerical simulation results suggest that the dynamic frictional weakening in the shallower segment plays a crucial role in the interaction between the deeper and the shallower segments.

Keywords: Slow tsunami earthquake, Megathrust earthquake, The Tohoku earthquake, Slip-rate, Slow slip

Japan Geoscience Union Meeting 2013
(May 19-24 2013 at Makuhari, Chiba, Japan)

SSS28-08 Room:303 Time:May 23 09:00-09:15

Fault modeling of the foreshocks of the 2011 Tohoku-oki earthquake based on near-field tsunami observation

Tatsuya Kubota[1*], Ryota Hino[1], Takeshi Iinuma[2], Yoshihiro Ito[1], Yusaku Ohta[1], Syuichi Suzuki[1], Daisuke Inazu[3], Tatsuhiko Saito[3], Yoshiyuki Kaneda[4]

[1]Graduate School of Science, Tohoku University, [2]International Research Institute of Disaster Science, [3]National Research Institute fo Earth Science and Disaster Prevention, [4]Japan Agency for Marine-Earth Science and Technology

We calculated the fault slip distribution of two large (Mw 7.3 on March 9 and Mw 6.5 on March 10) foreshocks of the 2011 Tohoku-Oki mainshock (Mw 9.0 on March 11) by inverting tsunami waveforms recorded by ocean bottom pressure gauges (OBPs) that had been deployed around the source area of the mainshock. These two foreshocks are the two largest foreshocks of the Mw9.0 mainshock. Both tsunami and coseismic vertical displacement of the seafloor were recorded clearly by OBPs. For the Mw 7.3 foreshock, the recorded tsunami amplitude and seafloor vertical displacement were up to 15 and 10 cm, respectively. During the Mw 6.5 foreshock, the vertical movement of 4 cm uplift was recorded at one of the OBP stations, and the tsunami with an amplitude of about 3 cm was recorded at several stations. In the tsunami waveform inversion for the both foreshocks, we use the same fault geometry based on Ito et al. (2005). As a first step of our analyses, we estimated the initial water surface height distribution through the inversion. The result is consistent with the pure reverse-fault type focal mechanism for both foreshocks. The results indicate that the main slip area of the Mw 7.3 foreshock is 40 km in length and 40 km in width and is located to the northwest of its epicenter. The maximum slip and the magnitude are estimated to be 1.0 m and Mw 7.3, respectively. The results indicate that the Mw 6.5 foreshock occurred about 20 km south of the epicenter of the Mw 7.3 foreshock and that the main slip area is 20 km in length and 40 km in width and is situated to the west of its epicenter. The maximum slip and magnitude are estimated to be 0.2 m and Mw 6.6. The calculated main slip area of the Mw 6.5 foreshock is located immediately south of the Mw 7.3 foreshock and is sandwiched between the epicenters of the Mw 7.3 foreshock and the mainshock. This indicates that the aseismic rupture propagated southwards sequentially. The postseismic slip of the Mw 7.3 foreshock likely caused aftershocks, which led to the second largest Mw6.5 foreshock. There were more aftershocks following the Mw 6.5 foreshock than Mw 7.3 foreshock. It is likely that this swarm of aftershocks triggered the initial rupture of the mainshock. The comparison between the tsunami sources of an M 7.0 earthquake off Miyagi in 1981 and the Mw 7.3 foreshock indicates that the Mw7.3 foreshock ruptured the same area of the 1981 event or that the area partially contained the rupture area of the 1981 earthquake.

Keywords: The 2011 off the Pacific coast of Tohoku earthquake, Foreshocks, Tsunami

Japan Geoscience Union Meeting 2013
(May 19-24 2013 at Makuhari, Chiba, Japan)

SSS28-09 Room:303 Time:May 23 09:15-09:30

Rupture Process of The 2011 Tohoku-Oki Earthquake Inferred by a Waveform Inversion Using 3D Green's Tensor Synthetics

Taro Okamoto[1*], Hiroshi Takenaka[2], Tatsuhiko Hara[3], Takeshi Nakamura[4], Takayuki Aoki[5]

[1]Dept. Earth Planet. Sci., Tokyo Institute of Technology, [2]Dept. Earth Planet. Sci., Kyushu University, [3]IISEE, Building Research Institute, [4]JAMSTEC, [5]GSIC, Tokyo Institute of Technology

The March 11, 2011 Tohoku-Oki earthquake (GCMT Mw9.1) generated strong ground motions and large tsunamis, and caused devastating damages in the northeastern Japan. Estimating the rupture process of this event is very important for understanding the geophysical condition of the generation of megathurust earthquakes and the mechanism of the excitation of the large tsunamis.

We present the rupture process analysis of the 2011 Tohoku-Oki earthquake by using a non-linear full-waveform inversion method in which the teleseismic and the strong motion seismograms are jointly used. We incorporate the effect of the near-source laterally heterogeneous structure on the synthetic Green's tensor waveforms because the solution can be erroneous one if the effect is not considered (e.g., if only a flat layered structure is used) [1]. For the teleseismic P-wave synthetics we use a 2.5-dimensional finite-difference method [2]. For the strong motion synthetics we use a full three-dimensional finite-difference method that incorporates topography, oceanic water layer, three-dimensional heterogeneity and attenuation. Our simulation is accelerated by the use of hundreds of GPUs used in parallel [3]. We use a GPU supercomputer, the TSUBAME-2.0 in Tokyo Institute of Technology.

As a preliminary analysis we computed Green's tensor synthetic waveforms for 31 teleseismic and 15 strong motion components. We used 640 GPUs of the TSUBAME supercomputer for the calculation of each strong motion synthetics. The inferred slip distribution has large slips near and around the JMA epicenter and has relatively less slips near the trench: the major rupture apparently migrate toward the north of the epicenter and the maximum slip is about 40 m. We will present results by incorporating more strong ground motion records and discuss the effect of the choice of the Green's tensor waveforms on the solutions.

[1] Okamoto and Takenaka, Earth Planets Space, 61, e17-e20, 2009.
[2] Takenaka and Okamoto, in Seismic Waves, Research and Analysis, ed. Kanao Masaki, Intech, 2012.
[3] Okamoto et al, in GPU Solutions to Multi-scale Problems in Science and Engineering, ed. D.A. Yuen et al., Springer, 2013.

Keywords: 2011 Tohoku-Oki earthquake, rupture process, 3D finite-difference method

Japan Geoscience Union Meeting 2013
(May 19-24 2013 at Makuhari, Chiba, Japan)

SSS28-10 Room:303 Time:May 23 09:30-09:45

2011 Tohoku earthquake: Unified source model and its rupture process

Yusuke Yokota[1], Kazuki Koketsu[1*], Yushiro Fujii[2]

[1]Earthquake Research Institute, University of Tokyo, [2]International Institute of Seismology and Earthquake Engineering, Building Research Institute

The devastating 2011 Tohoku earthquake was observed by dense networks of strong motion, teleseismic, geodetic, and tsunami. We performed checkerboard resolution tests for assessing the resolving power of the datasets obtained by the networks. From the results, we found that the individual datasets had only limited resolutions. In order to overcome these limitations, Koketsu *et al.* (2011) constructed the first version of the unified source model through a triple joint inversion of the teleseismic, strong motion, and geodetic datasets. Yokota *et al.* (2011) next performed a quadruple joint inversion of all the four datasets to determine the 1.5th version of the unified source model.

Although the above inversions were performed using one-dimensional Green's functions, we constructed the second version of this unified source model inferred taking three-dimensional (3-D) velocity structures into consideration. To achieve this, we calculated the 3-D Green's functions using the finite element method. We first inverted each of the datasets separately, and then performed a triple joint inversion of the strong motion, geodetic, and tsunami datasets for the second version of the unified source model. The teleseismic dataset was excluded, because the checkerboard tests had shown its low resolving power.

The total seismic moment in the second version was calculated to be 4.2 x 10^{22} Nm, which yielded M_W 9.0. This model revealed that the first rupture expanded at a slow speed of 2.0 km/s to the Japan Trench after small rupture in the initial 40 s. The second rupture began 20 s later at the slowest speed of 1.7 km/s and became dominant with the largest slip of 36 m. The third rupture then played the leading role, propagating southward at a speed of 2.5 km/s. The slow rupture speed and first rupture to the Japan Trench can explain the features of the disaster by the earthquake.

Keywords: 2011 Tohoku earthquake, unified source model, rupture process

Japan Geoscience Union Meeting 2013
(May 19-24 2013 at Makuhari, Chiba, Japan)

SSS28-11 Room:303 Time:May 23 09:45-10:00

Similarities and differences of the 1952 and 2003 Tokachi-oki earthquakes

Hiroaki Kobayashi[1*], Kazuki Koketsu[1], Hiroe Miyake[1], Hiroo Kanamori[2]

[1]ERI, Univ. Tokyo, [2]Caltech

Along the Kuril Trench off the Pacific coast of Hokkaido, many destructive earthquakes have occurred. Among those, the 1952 Tokachi-oki earthquake (41.706^{o}N, 144.151^{o}E, depth: 52 km) and the 2003 Tokachi-oki earthquake (41.779^{o}N, 144.079^{o}E, depth: 45 km) were very close to each other and their magnitudes (M_{JMA} 8.2 and M_{JMA} 8.0) were also close to each other. Therefore, it is highly possible that these two earthquakes were characteristic plate-boundary earthquakes.

The source process of the 1952 earthquake was analyzed using strong-motion data (Yamanaka and Kikuchi, 2003) and tsunami data (Hirata *et al*., 2003; Satake *et al*., 2006). However, the slip distributions obtained by those studies were different from each other, because many strong-motion seismograms went off scale after the S-wave arrival so that sufficient data length was not available for the strong-motion data.

In this study, we performed joint inversions of teleseismic data which were recorded with enough lengths and strong-motion data to analyze the whole rupture process of the 1952 earthquake. We also analyzed the 2003 earthquake with the same methods to examine the differences and similarities of these two earthquakes.

For the dataset of the 1952 earthquake, we collected the copies of seismograms which were recorded by historical seismographs, and digitized them. For the dataset of the 2003 earthquake, we used teleseismic data from IRIS-DMC and strong-motion data from K-NET. When we selected the stations, we took care to include the stations which are identical to, or nearby, those of the 1952 earthquake.

We first compared the datasets of the two earthquakes. The results revealed that the 1952 earthquake was composed of two large events and the data from the first event look similar to the ones of the 2003 earthquake. In addition, the initial parts of data suggest that the 1952 earthquake was preceded by a small event.

Secondly, we performed joint inversions of the teleseismic and strong-motion data. The results showed that the 1952 earthquake was composed of two large events as shown in the above comparison. The rupture first propagated to the western part and then to the eastern part. The moment rate function of the western event was similar to the one of the 2003 earthquake and their rupture areas almost overlapped with each other.

In summary, the western event of the 1952 earthquake and the 2003 earthquake are characteristic great earthquakes, but the eastern event and the small event are specific only to the 1952 earthquake.

Keywords: source process, inversion, the 1952 Tokachi-oki earthquake, the 2003 Tokachi-oki earthquake, characteristic earthquake

Japan Geoscience Union Meeting 2013
(May 19-24 2013 at Makuhari, Chiba, Japan)

SSS28-12 Room:303 Time:May 23 10:00-10:15

Rupture process of the 2004 Sumatra earthquake using teleseismic body waves

Masahiro Yoshimoto[1*], Yoshiko Yamanaka[1]

[1]Environmental Studies, Nagoya Univ

The 2004 Sumatra earthquake was one of the largest earthquakes in recorded history, and had a ˜1500 km long rupture of more than 500 seconds duration. To describe the whole rupture process of this earthquake, records of at least 500 seconds in duration were required for analysis. However, it is difficult to compute later phases using traditional rupture process analysis based on ray theory, which often uses the duration of analysis before the arrival of the later phases. In addition, such methods never compute a long period phase like a W phase. Although Ammon et al., (2005) inverted the rupture process using the Spectral Element Method which can compute the phases discussed above, they used body and surface waves at slightly long period range from 20 to 2000 seconds.

This study analyzes the rupture process of this earthquake using the Green's functions calculated by the Direct Solution Method (DSM). The Green's functions were computed up to 1 Hz for IASP91 model (Kennett and Engdahl, 1991) using the DSM software developed by Dr.Takeuchi (http://www.eri.u-tokyo.ac.jp/takeuchi/software/). The slip distributions were also determined using the waveform inversion scheme presented in Kikuchi et al. (2003).

The main results of waveform inversion are as follows: the moment magnitude, Mw, was determined to be 9.1; the source duration was 500 seconds; and the rupture velocity was 2.5-3.0 km/s. The synthetic seismograms matched well with the observations including the later phases and W phase. The largest slip area was estimated to be located from south west to west of the Sumatra islands, the second and third largest slip areas were estimated to be around the Nicobar islands, but almost no slip was found around the Andaman region.

Japan Geoscience Union Meeting 2013
(May 19-24 2013 at Makuhari, Chiba, Japan)

SSS28-13 Room:303 Time:May 23 10:15-10:30

Short recurrence intervals of repeating earthquakes in the Tonga subduction zone

Shimon Abe[1*], Satoshi Ide[1]

[1]Dept. EPS, Univ. Tokyo

The Tonga subduction zone is characterized by high seismicity and fast convergence rates exceeding 20 cm/year with a wide variation along the trench. We searched repeating earthquakes in this region and identified several sequences.

We selected 1399 M $>$ 5 events with the depth shallower than 60 km occurred from 1991 to 2011 in the ANSS global earthquake catalog. For all events, broadband seismograms at about 27 stations were downloaded from IRIS DMC, and bandpass filtered in 0.02 - 4Hz. For each pair of two events, we computed a cross-correlation function between vertical seismograms recorded at the station CTAO, Australia, for 800 s time windows around the theoretical S arrival times. We consider two events are repeating when the maximum of the cross-correlation function is larger than 0.9. Through this procedure and manual inspection of recurrence intervals, we identified 45 repeating earthquakes in 11 sequences. Almost all events have a low-angle thrust mechanism and for most sequences, the difference of relative S arrival times between stations are less than 0.5 s, suggesting the proximity of source regions.

The recurrence intervals of these events are very short despite their large size. For example, five M6 earthquakes occurred in 1993-2011, with the average recurrence interval of about 4.3 years. After the normalization of recurrence intervals using the scaling law of Nadeau and Johnson (1998), we found that the recurrence intervals are yet short, compared with those estimated in other regions such as northeastern Japan subduction zone and Parkfield, California. This difference can be explained by the different convergence rates.

Keywords: repeating earthquake, Tonga subduction zone

Japan Geoscience Union Meeting 2013
(May 19-24 2013 at Makuhari, Chiba, Japan)

SSS28-14 Room:303 Time:May 23 10:30-10:45

Earthquake depth estimations in the Po Plain (North Italy) using teleseismic data: influence on stress drop.

Jean Letort[1*], Massa Marco[3], Cotton Fabrice[1], Guilbert Jocelyn[2], Drouet Stephane[1], Pacor Francesca[3], Traversa Paola[4]

[1]ISTerre Universite de Grenoble 1, CNRS, F-38041 Grenoble, France., [2]CEA/DAM/DIF, F-91297 Arpajon Cedex, France., [3]Instituto Nazionale di Geofisica e Vulcanologia, Milano, Italy., [4]EDF, Aix en Provence, France

On May 2012, the central part of the Padano-Emiliana Plain (North Italy), has been shocked by a dramatic sequence of earthquakes, with higest Mw 6.0. These events were very shallow (˜ 5-10 km) with low stress drops and large ground-motions amplitude have been observed in the fault area. On the opposite, on the last 25th and 27th January other two deeper moderate earthquakes (either with Mw 4.9) occurred in the same area (south of Parma). These two events made very few damages and no victims, but have been felt also far from the source, which could be explained by their important focal depths (33 and 65 km respectively). Hence, a study of depth influence on seismic properties is of great interest. However, Po plain is a very complex area, the largest alluvial basin of northern Italy, characterized by anomalous propagation dues to the variable thickness of quaternary alluvium and with complex Moho discontinuities (Appenines Moho, Alpine Moho and Ligurian Moho): depth estimation can be sometimes challenging. Recent seismicity studies proposed that a deeper subducting slab of Adriatic lithosphere could occur as well in this area and the question about the depth estimation resolution remains open.

Based on teleseismic dataset, we have used coherent depth phases detected on CTBTO arrays (comprehensive-test-ban treaty-organization), using cepstral methods as well as focal mechanism estimations from genetic algorithm inversions to constrain the depths of all recent events above magnitude 3.8 in this area. The use of the teleseismic records gives the opportunity to reduce uncertainties due to complex crustal propagations during regional depth estimations. Moreover, pmP reflexions, observable on some teleseismic records, prove that, at least one event, (January 27, 2012) occurred below the Moho discontinuity, strengthening the hypothesis of the active slab.

Then, we have focused on characterizing the link between depth and stress drop, as it is a crucial parameter for ground motion prediction models. Hence, In addition of our new improved depth catalog, good stress drops evaluations are needed. These stress drops have been extracted from source spectra (magnitudes and corner frequencies, assuming Brune 's model), using the regional North Italy dataset collected in the last years by the strong-motion network (RAIS, INGV). We have used an iterative Gauss-Newton method developed by Drouet et al. (2011), which aims to separate source, sites effects and propagation contributions in the acceleration spectra. Inverted attenuation parameters are similar to those estimated by Castro et al. (2013) and sites effects have been checked to be coherent with the H/V profiles from the RAIS web site (http://rais.mi.ingv.it/), which strongly validate the isolated source spectra, thus, the associated stress drops. Finally, depth and stress drop are shown to be strongly correlated as depth events show high stress drop. Hence, in the global aim to predict ground motions, it seems that depth should be taken account in a more systematic way; especially as new seismic equipments (for instance CTBTO arrays) afford now better resolution for this crucial parameter.

Keywords: depth, stress drop, teleseismic, Po Plain, parametric inversion, corner frequency

Japan Geoscience Union Meeting 2013
(May 19-24 2013 at Makuhari, Chiba, Japan)

SSS28-15 Room:303 Time:May 23 11:00-11:15

Relationship between fc and Mo for AE from continuous and broadband records under a triaxial compressive condition

Nana Yoshimitsu[1*], Hironori Kawakata[2], Naoki Takahashi[3]

[1]Earthquake Research Institute, the University of Tokyo, [2]Ritsumeikan University, [3]Sumitomo Mitsui Construction Co., Ltd.

Micro fractures observed in laboratory experiments (acoustic emission; AE) have been studied to investigate a detailed faulting process [e.g., Yanagidani et al., 1985; Lockner et al., 1991]. To apply findings obtained in laboratory to field scales, it should be revealed that whether source characteristics of micro fracture is common with natural earthquakes or not due to large differences in scale. Seismic moment and corner frequency are fundamental parameters that characterize the source properties of the earthquake rupture. Down to events having a moment magnitude about -4, seismic moment thought to be proportional to cube of corner frequency [e.g., Abercrombie, 1995; Kwiatek et al., 2011]. However, it is still unclear whether AE size events also satisfies this relationship.

Previously, PZT elements which have narrow frequency ranges were often used as AE sensors, but their record were unsuitable for source parameter estimation. To overcame this problem, Sellers et al. [2003] tried to record AE with broadband transducers under a uniaxial rock fracture experiment. Though they indicated that the source parameters of AE events satisfied the same scaling relationship as that of natural earthquakes, the scaling relationship of AE themselves was still unconfirmed. In this study, we achieved multi-channel, broadband and continuous recording of AE and estimated source parameters of them in a higher accuracy.

We mounted nine broadband transducers (sensitive range: 100 kHz - 2000 kHz) that were hermetically sealed with metallic cases around a cylindrical Westerly granite sample (100 mm in height and 50 mm in diameter). Sampling rate was 20 MS/s per channel. Loading was continued until differential stress decreased (46 MPa) after the peak strength (296 MPa), under a confining pressure of 10 MPa.

We focused on two clusters of events (around 1000 events) which occurred after the peak strength was reached. The hypocenters of each event in a cluster located less than 2 mm apart, and correlation coefficients exceeded 0.80 for four or more channels in the cluster. After the spectral correction, we obtained displacement spectra for S waves. We estimated corner frequency and seismic moment for events with sufficiently high signal-to-noise ratios.

Corner frequencies and seismic moments obtained from AE events in each cluster (moment magnitude of events are around -8 to -7) satisfied the scaling relationship that applies to natural earthquakes. In addition, they were found to satisfy the same scaling relationship for AE events alone. Stress drops of events were distributed from 0.4 MPa to 12 MPa.

This result indicates self-similar relationship between micro fractures in laboratory and natural earthquakes.

Keywords: corner frequency, seismic moment, scaling, AE, rock fracture experiment

Japan Geoscience Union Meeting 2013
(May 19-24 2013 at Makuhari, Chiba, Japan)

SSS28-16 Room:303 Time:May 23 11:15-11:30

Microruptures concentrating on pre-existing planes at 1 km depth in a South African gold mine and their high b-values

Makoto Naoi[1*], Masao Nakatani[1], Kenshiro Otsuki[2], Yasuo Yabe[2], Thabang Kgarume[3], Gilbert Morema[4], Joachim Philipp[5], Sifiso Khambule[6], Thabang Masakale[6], Luiz Ribeiro[4], Hirokazu Moriya[2], Osamu Murakami[7], Shigeki Horiuchi[8], Hironori Kawakata[7], Nana Yoshimitsu[7], Koji Miyakawa[1], Atsushi Watanabe[1], Tony Ward[4], Ray Durrheim[3], Hiroshi Ogasawara[7]

[1]Univ. of Tokyo, [2]Tohoku Univ., [3]CSIR, [4]Seismogen, [5]GMuG, [6]OHMS, [7]Ritsumeikan Univ., [8]Home seismometer corp.

We deployed an Acoustic Emission (AE) sensor array, which can detect small ruptures down to Mw -5, at 1 km depth in the Cooke 4 shaft (previously known as Ezulwini mine) in South Africa, where up to Mw 3 class earthquakes are indued by mining of a planar gold reef. Naoi et al. [2012; SSJ fall meeting, poster] determined hypocenters by an automatic picking program [Horiuchi et al. 2011] and estimated Mw for 365,237 events. Ninety percent of those were located near mining fronts (hereinafter referred to as stope cluster), whereas most of the remainder belonged to planar clusters apart from the stope-cluster (hereinafter referred to as planar cluster). Naoi et al. [2012] investigated the stope-cluster AEs and showed that they obeyed the GR law with b = 1.3 from Mw -3.7 to 0. The b-value did not depend on time from blasting, even for 0-1min after blasts. Naoi et al. [2012] also confirmed the size distributions of earthquakes detected by mine's seismic network, which were dominated by stope-cluster events, obeyed the GR law with b = 1.3 from Mw -1.2 to 1 (To extract a sufficient number of events, catalogue for longer period and larger volume were used for the mine's seismic network). These suggest that stope-cluster events compose a population obeying the GR law with b = 1.3 between Mw -3.7 and 1.

The present study focus on planar-cluster AEs. We identified 7 planar clusters whose spatial extents were 10 - 80 m, which were located 20 - 70 m away from the mining front and were composed of 314 - 8667 AEs. Position and attitude of one of these clusters was consistent with a large geological fault (named Zebra fault) surrounding which our AE network was deployed. Also, corresponding weak planes (seemed to be joints) were found in tunnel for two other clusters. The remainders are thought to be related to unknown pre-existing weak planes that were not accessible for observation. Because event rates in these planar clusters were nearly constant during the analysis period and because no large earthquake occurred around them whose rupture extent could reach the extents of these clusters since 2009, when mining was started around the AE array, AEs of the planar clusters were judged to be steady activities, not aftershocks of large earthquakes. Relocated hypocenters of these planar clusters by Double Difference method [Waldhauser and Ellsworth, 2000] revealed that their distribution is so sharp that most hypocenters were aggregated within a thickness of 50 cm at the narrowest, sometimes event delineating stepovers and branches. These clusters were unrecognizable unless very small AEs were observed, because the 99.8% of the AEs in these planar clusters were smaller than Mw -2. Particularly, the maximum event in the planar cluster delineating Zebra fault was only Mw -3.0. The size distributions of the planar clusters followed the power law, and their slopes (b-value) were 1.38 to 2.19, which are higher than b-value of stope-cluster (b = 1.3).

Strong planar concentration of planar-cluster AEs observed in the present study is not necessarily consistent with microearthquake activities around active faults (e.g., Liu et al. 2003; Hauksson 2010). In addition, b-values of planar-cluster AEs were significantly different from typically observed b-values for natural earthquakes, whereas b-value of stope-cluster AEs was similar to those of natural earthquakes. This may be interpreted that size distribution of stope-cluster AEs and natural earthquakes reflect size distributions of weak planes in a volume region, whereas planar-cluster AEs are "microruptures" reflecting microscopic irregularities of a macroscopic weak plane (e.g., roughness of a fault); that is, planar-cluster AEs represent a different population from microearthquakes in the usual sense.

Keywords: Acoustic Emission, seismicity, South African deep gold mine

Japan Geoscience Union Meeting 2013
(May 19-24 2013 at Makuhari, Chiba, Japan)

SSS28-17 Room:303 Time:May 23 11:30-11:45

Energy Partition to Gouge Generation during Stick-slip as Studied by a New Large Biaxial Friction Ap

Tetsuhiro Togo[1*], Eiichi Fukuyama[2], Futoshi Yamashita[2], Kazuo Mizoguchi[3]

[1]Institute of Geology, China Earthquake Administration, [2]National Research Institute for Earth Science and Disaster Prevention, [3]Central Research Institute of Electric Power Industry

To determine how much of the frictional energy consume in generating fault gouge and breccia is important because this fraction will affect the energy used for frictional heating which in turn can affect the mechanical properties of a fault during seismic fault motion. In addition, it is geologically important to understand the formation and developing process of the mature fault zones.

We have used the large biaxial machine newly constructed in National Research Institute for Earth Science and Disaster Prevention (NIED), Tsukuba (Fukuyama et al. 2012 and Yamashita et al. 2012). This machine is developed to bridge a scale-gap between natural earthquakes (~km) and conventional laboratory experiments (~mm). The machine is built on the shaking table and used the hydraulic actuator of the table as the shear loading jack.

We have conducted seven biaxial friction experiments on Indian gabbro at average slip rates of 1.09 to 110 mm/sec, at normal stresses of 0.66 to 1.32 MPa and with displacements to around 0.42 m. Rectangular specimens of $1.5 * 0.5 * 0.5$ m and $2.0 * 0.5 * 0.5$ m with the surface irregularity less than 24 microns are used. The same specimens are repeatedly used in all experiments but the generated gouge was collected in each experiment by using the brush to measure the surface energy.

All experiments showed violent stick slip events except for the first run (v = 1.09 mm/s, normal stress = 0.67 MPa) where a stick-slip amplitude increased from small to moderate values with increasing displacement. Overshooting of shear stress occurred during some stick-slip events at slip rates of 10 mm/s and 100 mm/s; that is, shear stresses dropped down to negative values during some stick-slip events. The entire stiffness of the apparatus and shaking table was determined as $1.19*10^8$ N/m by using shear force drop (dF) and the displacement during slipping stage (dD) in each stick-slip event suggested by Shimamoto et al. (1980). This value is consistent with the quasi-static analysis.

The energy fraction of the gouge generation is determined by the surface energy of gouge divided by the frictional energy during each experiment (Togo and Shimamoto, 2012). Specific frictional energy in each experiment was obtained by the integration of the shear stress multiply displacement and the values were 0.18 to 5.16 MJ/m^2. Total surface energy of generated gouge in each experiment (E_A) was obtained the following equation.

$E_A = A_{BET} * r * m$

Where A_{BET} is the specific surface area of generated gouge, r is the surface free energy and m is the mass of the generated gouge. Specific surface area was measured by the BET surface area using a BELSORP-mini made by BEL Japan, Inc. with nitrogen as adsorbate. Specific surface area of the generated gouge showed high value of 5.29+-0.59 m^2/g at the first two experiments and it decreased with the increasing of the cumulative displacement to around 2.20+-0.49 m^2/g and total surface energy of generated gouge was 37.3 to 627.0 J. Results show that grain crushing absorbed only $9.63*10^{-4}$ to $1.39*10^{-1}$ % of frictional work. Thus, host rock wearing and gouge generation is unlikely to be an important energy sink at least for mature faults with well-developed slip zone.

Japan Geoscience Union Meeting 2013
(May 19-24 2013 at Makuhari, Chiba, Japan)

SSS28-18 Room:303 Time:May 23 11:45-12:00

Numerical analysis of failure of soil ground due to surface loading and generation of vibration induced by the failure

Akira Asaoka[1], Shotaro Yamada[2*], Toshihiro Noda[2]

[1]Association for the Development of Earthquake Prediction, [2]Nagoya University

In modern soil mechanics/geo-mechanics, the failure of soil ground has been analyzed as a progressive failure, in which elasto-plastic nature is introduced for the soil behavior. The main target of the analysis is the prediction of both the shape and the location of strain localization area in the ground and they intend to observe, through computation, how the strain localization area develops progressively with time and with space. The analysis is then somewhat different from the conventional slip failure analysis in which the shape and the location of failure zone and/or slip line are usually considered as given conditions for the analysis[1), 2)].

In this study, the so called ”bearing capacity problem” in soil engineering is newly analyzed as an example problem of the progressive failure of soil ground, in which vibration behavior of the ground is first observed, through computation, during the whole procedure of progressive failure. The numerical analyses are performed using the soil-water coupled finite deformation analysis code ***GEOASIA***[3)] that mounts the SYS Cam-clay[4)] elasto-plastic soil model on it. In the analysis, since the rate type equation of motion is precisely time-integrated, then progressive failure will be completely analyzed as a nonlinear dynamic problem.

First considered was the case of ”displacement control loading” in which loading to the ground is applied with constant rate of displacement of foundation. In this case, the soil ground exhibited localization of deformation and formation of a circular arc-shaped slip failure. At the same time ”load reduction” was also observed with the development of failure zone. To the same soil ground, surface load was next applied by the ”load control” method. In this case, after the applied load reached the peak load, the soil ground suddenly failed and dynamic motions with acceleration were observed at the foundation under the same amount of applied load. Very much irregular vibration was also observed in surrounding ground due to the ”shock” of the failure[5)]. In the vibration, very high frequency components were found to dominate, the reason for which will be due to the small scale of foundation. Focused on this point, the analysis objects were next scaled up 300 times big (from 8m high and 96m wide to 2.4km high and 24.8km wide). In this case, the dominant period of the vibration acceleration in surrounding ground shifted from about 0.2-0.3 seconds to about 5-8 seconds, keeping the amount of maximum acceleration almost the same. The descent of shear stress in slip/failure region that led to both the ”load reduction” and the dynamic motion of foundation will be delivered later.

Recently, geo-materials have been obtained from deep subduction zone of huge plates. Although the authors have not seen such geo-materials yet, they intend to make research works that describe the change of elasto-plastic properties of such geo-materials that should have occurred due to the subduction zone slip failure using the computational elasto-plastic geo-mechanics.

References:

1) Asaoka, A., Nakano, M. and Noda, T. (1994): Soil-water coupled behaviour of saturated clay near/at critical state, *Soils and Foundations*, **34(1)** , 91-106.

2) Noda, T., Yamada, S. and Asaoka, A. (2005): Elasto-plastic behavior of naturally deposited clay during/after sampling, *Soils and Foundations*, **45(1)**, 51-64.

3) Noda, T., Asaoka, A. and Nakano, M. (2008): Soil-water coupled finite deformation analysis based on a rate-type equation of motion incorporating the SYS Cam-clay model, *Soils and Foundations*, **48(6)**, 771-790.

4) Asaoka, A., Noda, T., Yamada, E., Kaneda, K. and Nakano, M. (2002): An elasto-plastic description of two distinct volume change mechanisms of soils, *Soils and Foundations*, **42(5)**, 47-57.

5) Noda, T., Xu, B. and Asaoka, A. Acceleration generation due to strain localization of saturated clay specimen based on dynamic soil-water coupled finite deformation analysis, *Soils and Foundations*, to be submitted.

Keywords: progressive failure, vibration, soil ground, elasto-plastic geo-mechanics, inertial force

SSS28-18 Room:303 Time:May 23 11:45-12:00

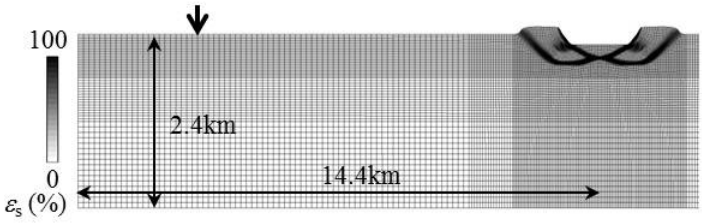

Fig. 1. Failure of ground with strain localization

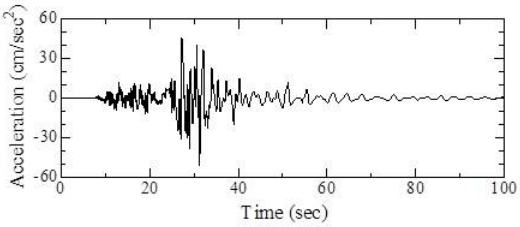

Fig. 2. Vibration in surrounding ground due to the shock of failure (at the point indicated by the arrow in Fig. 1.; vertical direction)